JPn

Neuroscience

The Journal of Physiology

Calcium-buffering effects of gluconate and nucleotides, as determined by a novel fluorimetric titration method

Andrew Woehler[1,2], Kun-Han Lin[1] and Erwin Neher[1,2]

[1]*Max-Planck-Institute for Biophysical Chemistry, Göttingen 37077, Germany*
[2]*DFG-Research Center for Nanoscale Microscopy and Molecular Physiology of the Brain (CNMPB), Göttingen 37073, Germany*

Key points

- The efficiency of neurotransmitter release is influenced by the presence of Ca^{2+} binding molecules.
- In this study we show that the use of gluconate as the dominant anion in pipette filling solutions, together with the presence of ATP and GTP, influences the efficiency of Ca^{2+}-mediated release during whole cell patch clamp measurements in the Calyx of Held.
- We introduce a novel fluorimetric titration procedure for low-affinity calcium dyes, such as Fura2FF, that allows us to determine the calcium binding ratios of several commonly used pipette solutions.
- These results explain the influence of gluconate and nucleotides on neurotransmitter release, provide guidelines for calibrating pipette solutions and calcium indicators, and may provide a basis for studying the coupling between calcium sensors and sources.

Abstract Significantly more Ca^{2+} influx is required for eliciting release of neurotransmitter during whole cell patch clamp recording in the Calyx of Held, when gluconate with 3 mM free ATP is used as pipette filling solution, as compared to a methanesulfonate-based solution with excess Mg^{2+}. This reduction in efficiency of Ca^{2+} in eliciting release is due to low-affinity Ca^{2+} binding of both gluconate and ATP^{2-} anions. To study these effects we developed a simple fluorimeteric titration procedure, which reports the dissociation constant, K_D, of a given Ca^{2+} indicator dye, multiplied by 1 plus the sum of Ca^{2+} binding ratios of any anions, which act as low-affinity Ca^{2+} ligands. For solutions without Ca^{2+} binding anions we find K_D values for Fura2FF ranging from 11.5 ± 1.7 to 15.6 ± 7.47 μM depending on the dominant anion used. For Fura6F and KCl-based solutions we find $K_D = 17.8 \pm 1.3$ μM. For solutions with gluconate as the main anion and for solutions that contain nucleotides, such as ATP and GTP, we find much higher values for the product. Assuming that the K_D of the indicator dye is equal to that of KCl-based solutions we calculate the summed Ca^{2+} binding ratios and find a value of 3.55 for a solution containing 100 mM potassium gluconate and 4 mM ATP. Gluconate contributes a value of 1.75 to this number, while the contribution of ATP depends strongly on the presence of Mg^{2+} and varies from 0.8 (with excess Mg^{2+}) to 13.8 (in the presence of 3 mM free ATP). Methanesulfonate has negligible Ca^{2+} binding capacity. These results explain the reduced efficiency of Ca^{2+} influx in the presence of gluconate or nucleotides, as these anions are expected to intercept Ca^{2+} ions at short distance.

Introduction

Ca^{2+} binding anions, such as EGTA and BAPTA, are known to reduce the efficiency of Ca^{2+} influx in eliciting neurotransmitter release, if present in the intracellular milieu of presynaptic nerve endings (Adler *et al.* 1991; Eggermann *et al.* 2011). In fact, comparison of the differential effects of EGTA (a slow Ca^{2+} binder) and BAPTA (a rapid binder) have been used extensively to infer the spatial relationship between Ca^{2+} channels and Ca^{2+} sensors, as these two chelators intercept inflowing Ca^{2+} ions at very different mean diffusion distances. However, most intracellular solutions in patch clamp studies also contain nucleotides and many protocols use gluconate as the main intracellular anion. Both nucleotides and gluconate are known to display low affinity Ca^{2+} binding (Skibsted & Kilde, 1972), with ATP^{2-} being reported to be among the fastest Ca^{2+} ligands (Hammes & Levison, 1964). The presence of such anions might strongly influence release. However, such effects are difficult to anticipate theoretically, as binding activities depend on the specific composition of solutions and Ca^{2+} binding to ATP^{2-} is antagonized by Mg^{2+} and H$^+$. We therefore developed a simple fluorimetic titration procedure, based on the low affinity Ca^{2+} indicator dye Fura2FF, to determine the overall Ca^{2+} binding capacity of solutions, as they are typically used in whole-cell patch clamp recordings (pH 7.2, ionic strength 190 mM and room temperature). The method returns the product of the dissociation constant K_D of the indicator dye and the sum of Ca^{2+} binding ratios of all low-affinity Ca^{2+} binders (incremented by 1). Thus, in the absence of Ca^{2+} binders we obtain the K_D of the dye, which may be used for its calibration as a Ca^{2+} indicator. Changes in K_D upon the inclusion of Ca^{2+} binders can then be used to calculate the Ca^{2+} binding properties of the latter. This type of calibration does not use other Ca^{2+} buffers for reference, but is based exclusively on the Ca^{2+} standard used for titrations.

We examine two low-affinity Ca^{2+} indicator dyes, Fura2FF and Fura6F. For characterizing the influence of anions we determine the Ca^{2+} binding ratio of some of the commonly used pipette-filling solution anions such as isethionate, gluconate, glutamate, methanesulfonate and commonly used nucleotides (ATP and GTP). We point out the role of magnesium regarding the latter and also address the problem of contamination by Ca^{2+} in minimally buffered solutions. Although, in typical pipette solutions, free ATP as well as gluconate were found to contribute only little to the Ca^{2+} binding ratio, their effects on the nanodomain Ca^{2+} may be substantial due to very high Ca^{2+} binding rates. We therefore measured the Ca^{2+} dependence of neurotransmitter release in the Calyx of Held synapse for two variants of nucleotide-containing solutions: one with methanesulfonate as the main anion and an excess of Mg^{2+} over nucleotides and one with gluconate and an excess of ATP^{2-}. We find that 2.7 times more Ca^{2+} influx is required for eliciting release of a physiological amount of neurotransmitter when the latter solution is used.

Methods

Theory

The law of mass action for Ca^{2+} binding to an indicator dye with dissociation constant K_D which is present at a total concentration F_t states that the concentration of Ca^{2+}-bound dye, [CaF], is given by

$$[\text{CaF}] = F_t \cdot [\text{Ca}^{2+}]/([\text{Ca}^{2+}] + K_D) \qquad (1)$$

If there are anions present, which bind Ca^{2+} with low affinity, one can rewrite this equation in terms of total Ca^{2+} ([Ca^{2+}]'), which is free or else in rapid equilibrium with low affinity Ca^{2+} binders other than the sensor:

$$[\text{Ca}^{2+}]' = [\text{Ca}^{2+}] \cdot \left(1 + \sum \kappa\right) \qquad (2)$$

Here $\Sigma\kappa$ is the sum of all Ca^{2+} binding ratios. The Ca^{2+} binding ratios are given (in the limit of low Ca^{2+} concentration) as the ratios of total concentrations over their K_D values (Zhou & Neher, 1993). We will refer to [Ca^{2+}]' as 'apparent free calcium' in the text below. Inserting eqn (2) into eqn (1) and denoting $1+\Sigma\kappa$ by κ', we obtain

$$[\text{CaF}] = F_t \cdot [\text{Ca}^{2+}]'/([\text{Ca}^{2+}]' + K_D \cdot \kappa') \qquad (3)$$

The fraction of Ca^{2+}-bound dye, f_{bound}, which can be determined experimentally, is given by

$$f_{\text{bound}} = [\text{CaF}]/F_t = [\text{Ca}^{2+}]'/([\text{Ca}^{2+}]' + K_{0.5}) \quad (4)$$

Here, we introduced for simplicity of notation

$$K_{0.5} = K_D \cdot \kappa' = K_D \cdot \left(1 + \sum \kappa\right) \qquad (5)$$

where the subscript 0.5 indicates the half point of the titration. Equation (4) shows that f_{bound} is a function of $K_{0.5}$ and does not allow one to separately determine K_D and κ'.

However, in the actual titration we also often include BAPTA to compensate for contamination (see above). Therefore, we have to consider the equation

$$\text{Ca}_t = [\text{Ca}^{2+}]' + [\text{CaF}] + [\text{CaB}] \qquad (6)$$

where [CaB] is the Ca^{2+}-bound form of BAPTA, for which equations in analogy to eqns (1) and (3) hold. Therefore

$$\text{Ca}_t = [\text{Ca}^{2+}]' + \frac{F_t \cdot [\text{Ca}^{2+}]'}{[\text{Ca}^{2+}]' + K_{0.5}} + \frac{B_t \cdot [\text{Ca}^{2+}]'}{[\text{Ca}^{2+}]' + K_{0.5,\text{B}}}$$

$$(7)$$

To calculate a prediction of f_{bound} from eqn (4) for a given $K_{0.5}$ and Ca^{2+} contamination (assumed as free parameters in the subsequent least squares fit), $[Ca^{2+}]'$ must be calculated through an iterative procedure similar to that used by standard chelator programs, such as MaxChelator (Bers *et al.* 1994). As starting values we used $[Ca^{2+}]' = Ca_t$, and adjusted $[Ca^{2+}]'$ in subsequent steps by a fraction of the difference between the calculated value for Ca_t and the target value. Using 0.01 as the fraction value, the procedure is repeated until it converges on a pair of $[Ca^{2+}]'$ and Ca_t values consistent with eqn (7). We then used $[Ca^{2+}]'$ and the estimates for $K_{0.5}$ and Ca^{2+} contamination to evaluate the sum of the square difference between the f_{bound} predicted by eqn (4) and the experimental data. This process was repeated with updated estimates of $K_{0.5}$, Ca^{2+} contamination and $[Ca^{2+}]'$ until a least squares fit of eqn (4) to the titration data was achieved. The figures show measured values of f_{bound}, together with the fits plotted against $[Ca^{2+}]'$, as determined by the fits.

The calculations outlined above require an estimate of the $K_{0.5,B}$ of BAPTA. For most solutions we used a value of 0.22 μM (Zhou & Neher, 1993). This is, of course, not correct for solutions with $\kappa' >> 1$. In a few cases we therefore repeated the least square fit with κ', as obtained in the first run, entering $K_{0.5,B} = \kappa' \cdot 0.22$ μM. Applying this procedure iteratively, the $K_{0.5}$ of the indicator dye generally decreased by about 5% while the fitted contamination decreased by about 10%.

Solution preparation

For calcium titration measurements, 4 mM calcium solutions were prepared for all pipette solutions outlined in Table 1 using 1 M stock calcium solution (VWR International BVBA, Leuven, Belgium). Adjustment of added calcium to 2, 3, 5, 10, 15, 25, 50, 100, 250, 1000 and 2000 μM was performed through dilution of the 4 mM calcium solutions with the corresponding calcium-free solutions. Fura2FF (TEFLabs, Austin, TX, USA) or Fura6F (Molecular Probes, Eugene, OR, USA) was added to all solutions at a final concentration of 5 μM and 20–100 μM BAPTA was added to all solutions to chelate any contaminating calcium. In all solutions the KCl (or otherwise CsCl content) was adjusted to obtain the required ionic strength (190.9 or 150.9 mM, see Table 2). For calcium contamination measurements, all base solutions with 200 μM BAPTA were prepared from 100 mM BAPTA stock (Molecular Probes). Solutions with 5, 10, 20, 30, 50 and 100 μM BAPTA were prepared through dilution of the high BAPTA solution with the zero BAPTA base solutions. For the potassium isethionate-based solution an initial 750 μM BAPTA solution was prepared from 100 mM BAPTA stocks and dilutions to 500, 200, 100, 50, 30, 20, 10 and 5 μM were performed.

Chemicals used in the preparation of potassium gluconate, potassium glutamate, potassium isethionate and caesium methanesulfonate-based solutions were obtained from Sigma (St Louis, MO, USA). Caesium gluconate was made by titrating gluconic acid with CsOH to pH 7.0 (Sigma). Cold methanol (-20°C) was added to the mixture until the solution turned slightly opaque. For crystallization, the solution was stored overnight at 4°C. The next day, the crystals were filtered off, dissolved in a minimum amount of water and treated with activated charcoal. The mixture was filtered through a fluted filter and the resulting clear liquid was mixed with methanol and again crystals were precipitated. The caesium gluconate salt was filtered and dried overnight at 40°C in a drying oven. All other chemicals were obtained from Sigma, and Merck (Darmstadt, Germany). All solutions were prepared in plastic vessels to prevent leaching of ions from glass vessels. To prepare solutions for titration experiments, substances were dissolved with ultrapure Millipore water in plastic containers and adjusted to the required pH by adding 1 M KOH or 1 M HCl except that 1 M CsOH was used for caesium-based solutions.

Fluorescence spectroscopy

Excitation spectra were measured using 5 μl of sample solution placed in a 1 mm path-length quartz cuvette (uCuvette G1.0, Eppendorf, Hamburg, Germany) using a Fluoromax2 spectrofluorometer (Horiba Jobin Yvon Inc., Edison, NJ, USA). Excitation wavelength was scanned from 260 to 450 nm in 2 nm increments while emission was collected at 510 nm with a slit width of 10 nm and 0.5 s integration. Reference excitation spectra for free and bound Fura2FF were measured from solutions with 200 μM BAPTA and 50 mM added calcium, respectively. All titrations were performed in triplicate at room temperature (22–24°C).

Evaluation of inner filter effect

To evaluate the presence of an inner filter effect (Lakowicz, 2006) within the 1 mm path-length cuvette used in the titration experiments, a series of solutions with increasing Fura2FF concentration were prepared in the calcium-free iKCl base solution (see Table 1). Samples with Fura2FF concentration ranging from 0 to 20 μM in 2.5 μM increments were prepared through serial dilution of the 20 μM solution with the dye-free solution. Excitation spectra were measured as outlined above and the peak excitation intensity was evaluated as a function of dye concentration. The peak intensity was found to be proportional to the concentration through 10 μM Fura2FF, only above which was quenching due to the inner filter effect observed.

Data analysis

To correct for small differences in sensor concentration all spectra were normalized to the intensity of emission with excitation at the isobestic point of Fura2FF, 354 nm. The free and bound sensor fractions within a given sample were determined through linear unmixing of the excitation spectra with the free and bound reference spectra. The bound fraction was then fit as a function of apparent total calcium, along with information of the added BAPTA and sensor concentrations, to determine the $K_{0.5}$, the apparent free calcium concentrations, $[Ca^{2+}]'$, and calcium contamination present in the sample (see Theory). The 95% confidence intervals for a given set of fitted parameters were determined as previously described (Bates & Watts, 2008; Bonate, 2011) using the root mean square error of the fit, the t-value for 95% confidence limit, and the variance–covariance matrix determined from the QR decomposition of the Jacobian matrix (partial derivatives of the fitted function evaluated at a given set of fitted parameters). All analysis was performed using Matlab 7.12 (The MathWorks, Natick, MA, USA).

Electrophysiology

Brainstem slices were prepared from juvenile (post-natal day 9–11) Wistar rats of either sex in accordance with national and institutional guidelines as previously described (Lin *et al.* 2012). After decapitation, the whole brain was immediately immersed into ice-cold low Ca^{2+} artificial cerebrospinal fluid (aCSF) containing the following (in mM): 125 NaCl, 2.5 KCl, 3 MgCl$_2$, 0.1 CaCl$_2$, 10 glucose, 25 NaHCO$_3$, 1.25 NaH$_2$PO$_4$, 0.4 ascorbic acid, 3 *myo*-inositol and 2 sodium pyruvate, pH 7.3. The brainstem was glued onto the stage of a VT1000S vibratome (Leica, Wetzlar, Germany), and 200 μm-thick coronal slices containing the medial nucleus of the trapezoid body were collected. Slices were equilibrated for 30 min at 35°C in the same aCSF solution, except that the CaCl$_2$ and MgCl$_2$ concentrations were 2 and 1 mM, respectively. Thereafter, slices were kept at room temperature (22–24°C) for up to 4 h.

Patch clamp recordings were made from Calyx of Held terminals using an EPC-10 amplifier controlled by Pulse software (HEKA Elektronik, Lambrecht/Pfalz, Germany). Sampling intervals and filter settings were 20 μs and 4.5 kHz, respectively. Cells were visualized by differential interference contrast microscopy through a 60× water-immersion objective (numerical aperture 1.0; Olympus) using an upright Axioskop FS microscope (Zeiss, Oberkochen, Germany). All experiments were performed at room temperature. Patch pipettes were prepared from borosilicate glass (Science Products, Hofheim, Germany) and pulled on a P-97 micropipette puller (Sutter Instruments, Novato, CA, USA) with an open tip resistance ranging from 4 to 5 MΩ. Pipettes were coated with dental wax to minimize fast capacitive transients during voltage clamp experiments and to reduce stray capacitance. Access resistance (R_s) values were ≤20 MΩ. R_s compensation was set to 60–70% (2 μs delay).

For measuring membrane capacitance (ΔC_m), pipettes were filled with solutions containing either caesium gluconate with 3 mM excess ATP, caesium gluconate with 2 mM excess Mg^{2+} or caesium methanesulfonate with 2 mM excess Mg^{2+} (see Table 1). Pipette solutions were supplemented with 50 μM EGTA to compensate for any Ca^{2+} contamination. The bath solution was supplemented with 1 μM TTX, 1 mM 4-aminopyridine, and 40 mM tetraethylammonium chloride to suppress voltage-gated Na^+ and K^+ currents. C_m was measured and ΔC_m was estimated as described previously (Lin *et al.* 2011). Offline analysis was done with Igor Pro (Wave-Metrics, Lake Oswego, OR, USA). Electrophysiological data are given as mean ± SEM.

Results

Fluorimetric titration of low-affinity Ca^{2+} dyes without the use of Ca^{2+} buffers

Traditionally, calibration of Ca^{2+} indicator dyes is performed with the help of calibration buffers. Varying the ratio of Ca^{2+}-bound to free form of the calibration buffer (such as BAPTA or EGTA), defined concentrations of free Ca^{2+} ($[Ca^{2+}]$) are established. Measurements of fluorescence ratio for a range of solutions with different free $[Ca^{2+}]$ then allow one to obtain and analyse a calibration curve, for example for determining the dissociation constant of the indicator dye. This procedure meets with two problems when applied to indicator dyes with dissociation constants in the range 10–20 μM: (1) relatively high concentrations of low-affinity calibration buffers are required to overcome the effects of Ca^{2+} binding to the indicator dye; and (2) the properties of the calibration buffers have to be known for the specific composition of the given solution, which in turn may require a calibration of that buffer in that solution.

Since our aim is to measure free Ca^{2+} in the presence of relatively high concentrations of anions, and to determine whether these anions have some low-affinity Ca^{2+} binding capacity, we would have to titrate such anions in a second step after calibrating the indicator dye. It turns out that there is a straightforward way to obtain the same information in a single titration run without resorting to a calibration buffer. As shown in the Methods, one can readily obtain an apparent dissociation constant $K_{0.5}$ from the midpoint of a fluorimetric titration, which is the product of the actual concentration-based K_D and the Ca^{2+} binding ratio κ_P of the low-affinity anions in the solution (subscript P for 'pipette' solution). In this

Table 1. Solution composition and $K_{0.5}$ values

Solution	IS	pH	Nucleotides	Chemical composition	$K_{0.5}$ ($\pm$ 95% CI)
iKCl w Hepes	150.9	7.2	—	147.9 KCl, 10 Hepes	9.8 $\pm$ 1.1
iKCl w Hepes	190.9	7.2	—	187.9 KCl, 10 Hepes	13.8 $\pm$ 1.1
iKCl w Hepes	190.9	6.0	—	187.9 KCl, 10 Hepes	15.9 $\pm$ 1.3
iKCl w Hepes	190.9	5.0	—	187.9 KCl, 10 Hepes	72.6 $\pm$ 2.5
iKCl w Hepes w nucleotide	190.9	7.2	+	160.0 KCl, 10 Hepes, 5 Na_2-phosphocreatine, 4 ATP-Mg, 0.3 Na_2-GTP	27.9 $\pm$ 1.7
Potassium gluconate, IS150	150.9	7.2	+	20 KCl, 100 potassium gluconate, 10 Hepes, 5 Na_2-phosphocreatine, 4 ATP-Mg, 0.3 Na_2-GTP	48.4 $\pm$ 2.1
Potassium gluconate, IS150	150.9	7.2	+	60 KCl, 60 potassium gluconate, 10 Hepes, 5 Na_2-phosphocreatine, 4 ATP-Mg, 0.3 Na_2-GTP	41.1 $\pm$ 2.5
Potassium gluconate	190.9	7.2	+	60 KCl, 100 potassium gluconate, 10 Hepes, 5 Na_2-phosphocreatine, 4 ATP-Mg, 0.3 Na_2-GTP	62.8 $\pm$ 3.4
Potassium gluconate w/o nucleotide	190.9	7.2	—	87.9 KCl, 100 potassium gluconate, 10 Hepes	37.9 $\pm$ 1.7
Caesium gluconate	190.9	7.2	+	30 CsCl, 100 caesium gluconate, 30 TEA-Cl, 10 Hepes, 5 Na_2-phosphocreatine, 4 ATP-Mg, 0.3 Na_2-GTP	65.5 $\pm$ 3.2
Caesium gluconate, EX ATP	190.9	7.2	+	15 CsCl, 100 caesium gluconate, 30 TEA-Cl, 10 Hepes, 1 $MgCl_2$ 5 Na_2-phosphocreatine, 4 Na_2-ATP, 0.3 Na_2-GTP	229.2 $\pm$ 3.9
Caesium gluconate, EX Mg	190.9	7.2	+	24 CsCl, 100 caesium gluconate, 30 TEA-Cl, 10 Hepes, 5 Na_2-phosphocreatine, 4 ATP-Mg, 0.3 Na_2-GTP, 2 $MgCl_2$	49.0 $\pm$ 2.3
Potassium glutamate w/o nucleotide	190.9	7.2	—	87.9 KCl, 100 potassium glutamate, 10 Hepes	14.8 $\pm$ 1.4
Potassium isethionate w/o nucleotide	190.9	7.2	—	87.9 KCl, 100 potassium isethionate, 10 Hepes	15.6 $\pm$ 7.4
Caesium methanesulfonate w/o nucleotide	190.9	7.2	—	57.9 CsCl, 100 caesium methanesulfonate, 30 TEA-Cl, 10 Hepes	11.5 $\pm$ 1.7
Caesium methanesulfonate EX Mg	190.9	7.2	+	24.0 CsCl, 100 caesium methanesulfonate, 30 TEA-Cl, 10 Hepes, 5 Na_2-phosphocreatine, 4 ATP-Mg, 0.3 Na_2-GTP, 2 $MgCl_2$	ND

ND, not determined.

titration defined amounts of Ca^{2+} are added, using a calibrated Ca^{2+} standard. The accuracy of the resulting $K_{0.5}$ values depends only on the accuracy of that standard, on the accuracy of pipetting and of fluorescence readings. Problems of Ca^{2+} contamination of the solution will be addressed below.

Figure 1A shows the result of three such titrations using 'isotonic' KCl (iKCl) (three different pH values) and 5 μM Fura2FF (for exact composition of the solutions see Table 1). The solution also contained 20 μM BAPTA for compensation of contaminating Ca^{2+}. The 'apparent free Ca^{2+}' (see eqn (6) extends from 100 nM to 10 mM. The

Table 2. Contamination values

Solution	IS	pH	Added BAPTA (μM)	Fitted contamination (μM)
iKCl	190.9	7.2	20	9.16
iKCl	190.9	6.0	20	9.83
iKCl	190.9	5.0	20	22.8
iKCl	150.9	7.2	20	9.35
iKCl + nucleotides	190.9	7.2	20	15.0
Potassium gluconate	190.9	7.2	20	17.5
Potassium gluconate	150.9	7.2	20	18.0
Potassium gluconate – nuc	190.9	7.2	20	15.7
Caesium gluconate	190.9	7.2	50	48.6
Caesium gluconate +ATP	190.9	7.2	50	56.5
Caesium gluconate +Mg	190.9	7.2	50	46.1
Potassium glutamate	190.9	7.2	20	15.7
Potassium isethionate	190.9	7.2	100	71.4
Caesium methanesulfonate	190.9	7.2	15	12.3

ordinate is the 'Ca^{2+} -bound fraction' of the indicator dye, as defined in the Methods. A least-squares fit of eqn (4) to the pH 7.2 data points yields a value for $K_{0.5}$ of 13.8 μM. Independent measurements comparing solutions with 10 and 1 mM Hepes under tight observation of pH showed that 10 mM Hepes did not influence the result. Assuming, then, that Cl$^-$ does not bind Ca^{2+} we adopt the value of 13.8 μM for the dissociation constant of Fura2FF at pH 7.2 in a KCl-based medium.

Dependence of the dissociation constant on pH and ionic strength

Figure 1*A* also contains data for two additional pH values. Slight acidification to pH 6 has little effect. However, switching to pH 5 increases the $K_{0.5}$ by a factor of 5.26. The inset in Fig. 1*A* plots the K_D values together with a fit to the equation $K_{0.5} = K_D{}^* \cdot (1 + [H^+] \cdot K_H)$, assuming competition between Ca^{2+} binding and H$^+$ binding to the doubly deprotonated form of Fura2FF only, with values for $K_D{}^* = 13$ μM and $K_H = 3.23 \times 10^5$ M^{-1}. Here, [H] was calculated according to $[H] = 10^{0.13-\text{pH}}$ (the offset of 0.13 corrects for the activity coefficient of H$^+$, according to Martell & Smith, 1974).

Figure 1*B* compares two titration curves, both at pH 7.2 for two different values of ionic strength, which cover the range of ionic strengths typically used for whole cell patch clamp experiments. The dissociation constant decreases (by 29%) when decreasing ionic strength by 40 mM. The inset plots K_D values together with a fit according to eqns (11)–(14) of Bers *et al.* (1994), which are based on the

electrochemical theory of dilute electrolytes (Harned & Owen, 1958; Harrison & Bers, 1989). The data conform to the theory quite well, but the low range of ionic strength values prevents any further conclusions. Combining the fits of Fig. 1*A* and B, one arrives at an approximate dependence of $K_{0.5}$ on pH and ionic strength (I, in mol l^{-1}) according to

$$K_{0.5}(\text{pH}, I) = -7.69 \cdot 10^{-6} + 5.66 \cdot 10^{-\text{pH}}$$
$$+ 1.09 \cdot 10^{-4} \cdot I \qquad (8)$$

The underlying data were obtained at room temperature (22°C), and need to be corrected for temperature differences. Using eqn (10) of Bers *et al.* (1994) and an enthalpy of 4.04 kcal M^{-1}, as reported for dibromoBAPTA, we predict a 1.4-fold decrease in $K_{0.5}$ when changing to physiological temperature.

Apparent Ca^{2+} affinity of Fura2FF for solutions with a variety of major anions

The binding of a cation to an anionic ligand (such as a Ca^{2+} indicator dye) is influenced not only by ionic strength, but also by the nature of the major ions in solution (Bockris & Reddy, 1973). These effects are generally represented by activity coefficients in the sense that activity of an ion (for which physiochemical laws, such as the law of mass action, hold strictly) is assumed to be the product of the stoichiometric concentration and an activity coefficient. Since our titrations are based on concentrations, the 'stoichiometric K_D' which we obtain is actually a product of the true dissociation constant (K_D) – the Ca^{2+} binding ratios (see above) – and a term representing activity coefficients of the participating ions. The latter vary with ionic strength and also somewhat with the nature of the dominant anions and cations. Therefore, we expect the measured $K_{0.5}$ to vary somewhat between solutions with different main anions. Mean molal activity coefficients for simple sodium salts at 200 mM ionic strength vary typically by about 10–20% (Robinson & Stokes, 1959). Therefore, we expect $K_{0.5}$ (which is a product of K_D and κ_P, see above) to vary to that degree, even in the absence of Ca^{2+} binding to any of the anions present. Any deviations larger than that are interpreted as Ca^{2+} binding.

Figure 2*A* shows titration curves for solutions similar to those of Fig. 1*A*, except that 100 mM KCl was replaced by either 100 mM potassium isethionate, potassium glutamate, or caesium methanesulfonate (all at pH 7.2). Values for $K_{0.5}$ are 15.6 ± 7.4, 14.8 ± 1.4 and 11.5 ± 1.7 μM, respectively (see Table 1 for a summary of results, shown as $\pm$ the 95% confidence limits). We consider the differences between these three anions and chloride to be within the range, which can be attributed to activity effects (see also Discussion).

Anions with low-affinity Ca²⁺ binding

Potassium gluconate is often used as major anion in whole cell patch clamp experiments. However, Christoffersen and Skibsted (1975) reported an apparent K_D for Ca^{2+} binding of gluconate⁻ of 15.5 mM (Christoffersen & Skibsted, 1975). This would imply that 100 mM potassium gluconate in a pipette solution would contribute $100/15.5 = 6.46$ to its κ_P value. Likewise, most pipette solutions contain nucleotides, such as ATP^{2-} and GTP^{2-}, which have Ca^{2+} and Mg^{2+} binding capacity. We therefore measured $K_{0.5}$ for solutions containing these anions.

First, we considered solutions, which again are very similar to that of Fig. 1A. In one solution, iKCl + nucleotides, 27.9 mM KCl is replaced by 5 mM Na_2phosphocreatine, 4 mM MgATP plus 0.3 mM Na_2GTP. In the other two solutions, potassium gluconate and potassium gluconate + nucleotides, 100 mM KCl of each corresponding iKCl solution is replaced by potassium gluconate. Calcium titrations of these solutions are plotted in Fig. 2B and show that both replacements shift the curves rightwards. In the KCl solutions the $K_{0.5}$ is increased by a factor of 2.02 as a result of the presence of nucleotides and

in the case of gluconate it is increased by a factor of 2.75. These changes are much larger than expected for merely electrostatic interactions and probably reflect low-affinity binding of Ca^{2+} to these anions (see Discussion).

We also tested the effect of ionic strength on $K_{0.5}$ in potassium gluconate-based solutions by lowering KCl for a total change in ionic strength from 190.9 to 150.9 mM. We did so in two different ways, once reducing KCl content from 60 to 20 mM and once reducing both KCl and potassium gluconate content proportionally. As in the case of the chloride-based solution, the $K_{0.5}$ decreased, as expected by theory.

Caesium-based solutions

The measurement of Ca^{2+} currents in nerve terminals requires the blockade of all other current components. Replacement of K^+ by Cs^+ is often used as an effective blocker of K^+ channels. We therefore tested several solutions, which are exactly those used in patch clamp experiments, with caesium gluconate as the main constituent and nucleotides, Na^+-phosphocreatine and Hepes added (see Table 1 for exact composition). We
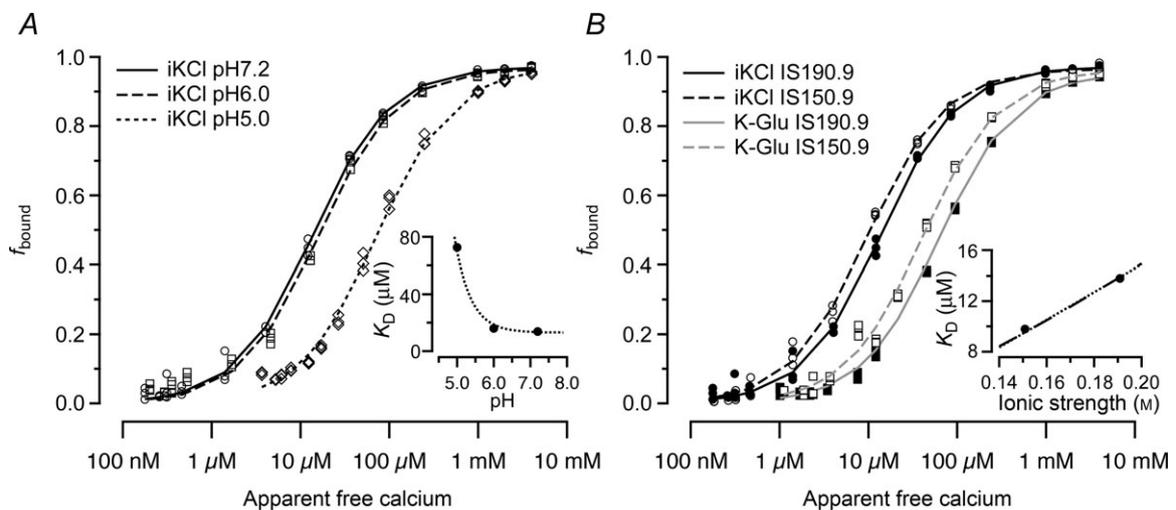
Figure 1. Effects of pH and ionic strength on the $K_{0.5}$ of Fura2FF
A, calcium titrations of three solutions of isotonic KCl solutions with 5 μM Fura2FF and pH values of 7.2 (circles), 6.0 (squares) and 5.0 (diamonds) were performed after initially chelating contaminating calcium with 20 μM BAPTA. The bound fraction of Fura2FF was plotted against the apparent free calcium. The least-squares fit of the bound fraction of Fura2FF from three measurements of pH 7.2 solution (continuous line) yielded a value for $K_{0.5}$ of 13.8 μM with initial Ca^{2+} contamination of 9.16 μM. Fitting the bound fractions from titrations of the pH 6.0 (dashed line) and pH 5.0 (dotted line) solutions yielded respective $K_{0.5}$ values of 15.9 ± 1.3 and 72.6 ± 2.5 μM and calcium contamination values of 9.8 and 22.8 μM. The insert shows a plot of $K_{0.5}$ *versus* pH with a theoretical curve according to: $K_{0.5} = 13 \cdot 10^{-6} \cdot (1 + 10^{(0.13-pH)}/3.1 \cdot 10^{-6})$. B, titrations of two solutions of isotonic KCl with 5 μM Fura2FF, pH 7.2, and different ionic strengths (IS) were performed. Fitting the bound fraction of Fura2FF as a function of added calcium for the solution with ionic strength of 190.9 mM (continuous line black) yielded a $K_{0.5}$ of 13.8 ± 1.1 μM, while decreasing the ionic strength to 150.9 mM (dashed black line) decreased the $K_{0.5}$ to 9.8 ± 1.1. Similar measurements were performed with potassium gluconate-based solutions and show a decrease in $K_{0.5}$ from 62.8 ± 3.4 to 41.1 ± 2.5 μM for the IS190 (solid grey line) and IS150 (dashed grey line) solutions, respectively. The insert shows a plot of $K_{0.5}$ of chloride-based solutions *versus* ionic strength with a theoretical curve according to Bers *et al.* (1994), constrained to pass through the data point at 0.19 mM. The theoretical curve is well approximated by $K_{0.5} = -6.891 \times 10^{-6} + 1.09 \times 10^{-4} I$, where I is the ionic strength.

were also interested in how far Mg^{2+} binding to ATP^{2-} would change the properties of the solutions. Therefore, we compared three cases: (1) the nucleotide composition, as used above for the potassium-based solution with an estimated free $[ATP^{2-}]$ of about 1 mM, (2) a solution with excess ATP^{2-} with free $[ATP^{2-}]$ of about 3.3 mM and (3) a solution with 1.7 mM excess Mg^{2+}, resulting in free $[ATP^{2-}] < 0.38$ mM (assuming $K_{D,Mg} = 0.02$ mM; Moisescu & Thieleczek, 1979).

Figure 3 plots titration curves for these three cases. In the case of 'normal' nucleotides the $K_{0.5}$ of 65.5 ± 3.2 μM is close to that of the equivalent potassium gluconate-based solution. Depleting free $[ATP^{2-}]$ by excess Mg^{2+} decreases this slightly to 49.0 ± 2.3 μM. However, increasing free ATP^{2-} increases $K_{0.5}$ to 229.2 ± 3.9 μM, which is 4.7 times higher than the value for depleted $[ATP^{2-}]$ and 16.7 times higher than the value for KCl-based solutions. This indicates that the contribution of 3 mM free ATP to κ_P is about 16 (see Discussion).

The influence of free $[ATP^{2-}]$ on Ca^{2+} sensitivity of neurotransmitter release

Given the strong effect of $[ATP^{2-}]$ on the Ca^{2+} binding ratio of pipette filling solutions, we studied neurotransmitter release in the Calyx of Held synapse using three solutions with different Ca^{2+} binding ratios. These included a caesium methanesulfonate-based solution with negligible Ca^{2+} binding, as well as two solutions with extreme differences in $[ATP^{2-}]$ (solution 'caesium

methanesulfonate ExMg', 'caesium gluconate ExATP', and 'caesium gluconate ExMg', Table 1). This was of interest, as estimates for the basal Ca^{2+} binding ratio of fixed Ca^{2+} buffers in the Calyx of Held range from 25 to 40 (Neher & Taschenberger, 2013), which indicates that the presence of 3 mM $[ATP^{2+}]$ and gluconate changes the Ca^{2+} binding ratio of dialysed cytosol substantially. Also, free $[ATP^{2-}]$ is known as a very fast Ca^{2+} binder (Hammes & Levison, 1964), which should be very potent in interfering with Ca^{2+} binding to the Ca^{2+} sensors of the neurotransmitter release apparatus. Indeed, when measuring capacitance changes in response to action potential-like stimuli, we observed substantial differences between the three solutions. The amount of Ca^{2+} influx during 3 ms ramp depolarizations was varied by varying the amplitudes of the depolarizations (Fig. 4A–C).

Figure 4D plots the observed capacitance changes, which are proportional to the number of vesicles released, as a function of the integral of the Ca^{2+} current transients. Maximum responses, depleting the whole rapidly releasing pool of vesicles, were obtained by 10 ms depolarizations to 0 mV (Lin *et al.* 2011). The data for the three solutions were fitted by Hill curves. The Hill coefficients were set to 2.6, which resulted in sigmoid-shaped curves, as is characteristic for the Ca^{2+} dependence of neurotransmitter release (Dodge & Rahamimoff, 1967). We used the Hill fits to calculate the Ca charge required to elicit a 20 fF response, which is close to what is released by an action potential. The resulting numbers were 0.5 pC for the
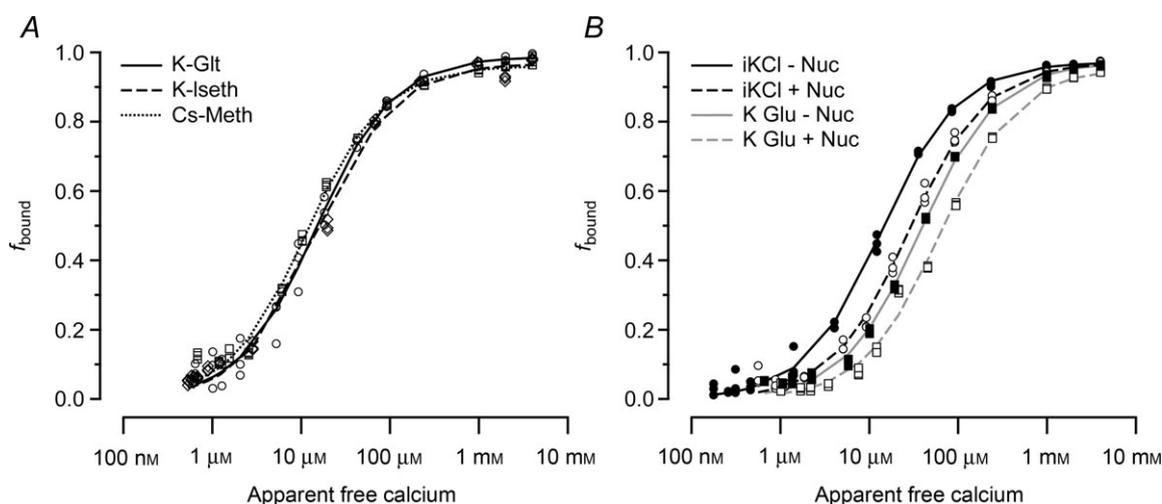
Figure 2. Effects of different dominant anions and nucleotides on the $K_{0.5}$ of Fura2FF
A, titration curves for solutions with 100 mM potassium glutamate, potassium isethionate or caesium methanesulfonate are indicated by the solid, dashed and dotted lines, respectively. Fitting the calcium-bound fraction of Fura2FF from three measurements of each solution yielded $K_{0.5}$ values of 14.8 ± 1.4 μM for the glutamate-based solution, 15.6 ± 7.5 μM for the isethionate solution and 11.5 ± 1.7 μM for the methanesulfonate solution. *B*, titrations of KCl and potassium gluconate-based solutions with and without nucleotides were performed. Fitting the bound fraction of Fura2FF in the iKCl solution without nucleotides (solid black line) present yielded a $K_{0.5}$ value of 13.8 ± 1.1 μM, while the presence of nucleotides (dashed black line) increased $K_{0.5}$ to 27.9 ± 1.7 μM. The fitted $K_{0.5}$ value for the potassium gluconate-based solution without nucleotides (solid grey line) was 37.9 ± 1.7 μM, while the presence of nucleotides (dashed grey line) increased $K_{0.5}$ to 62.8 ± 3.4 μM.

caesium methanesulfonate-based solution, 0.84 pC for the gluconate-based solution with excess Mg^{2+}, and 1.35 pC for the gluconate-based solution with excess ATP^{2-}.

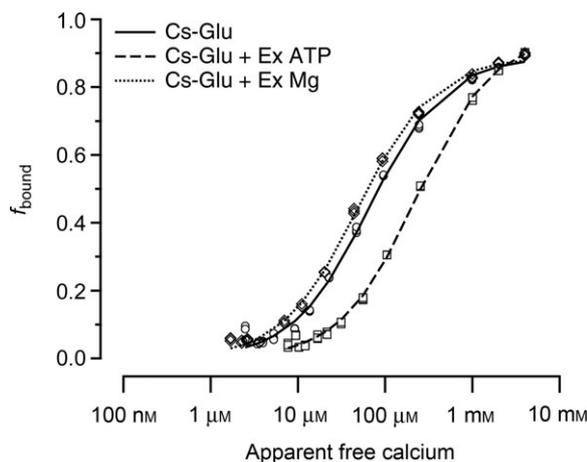## The handling of Ca^{2+} contamination

Titrating an indicator dye with a K_D around 15 μM requires solutions with free $[Ca^{2+}]$ ranging from about 1 μM to several hundred micromoles. Unfortunately solutions, even when prepared very carefully, have Ca^{2+} contamination in the range of a few to some tens of micromoles (Bers *et al.* 1994). At the low end these contaminations can be handled by using the (unknown) concentration of contamination as a free parameter in the fitting of titration curves (see Methods). For contaminations above 5 μM, however, the fitting becomes quite unreliable, as there are no low concentration points included in the fits. We therefore estimated contamination for all solutions used by a preliminary titration with BAPTA. We then added the required amount of BAPTA, thus determined, to 'neutralize' the contamination. Since the K_D of BAPTA is about 100 times smaller than the K_D of Fura2FF, BAPTA acts like 'negative Ca^{2+}', and the remaining difference between BAPTA and contamination can be readily handled in the fitting routine (see Methods). We would like to point out, however, that for *in vivo* experiments, neutralization of contaminating Ca^{2+} should be achieved with EGTA (and not BAPTA) to avoid effects on the Ca^{2+} nanodomain in the case of slight over-compensation. We found that our K^+-based solutions have typically 10–15 μM contamination, whereas caesium gluconate, for instance, has up to 50 μM contamination. Values for contamination are given in Table 2. In caesium gluconate solutions the apparent fraction of bound Ca^{2+} at saturating total Ca^{2+} stayed below the value typically observed for other solutions. We attribute this to the likely presence of metal ions other than Ca^{2+}, which may have higher affinity than Ca^{2+}, but lower fluorescence yield. To test this assumption we titrated caesium gluconate in the presence of 4 mM Ca^{2+} with TPEN, a chelator with very high affinity for heavy metal ions (Arslan *et al.* 1985), and found only a slight increase in maximum fluorescence compatible with the presence of about 2–5 μM heavy metals.

Comparison between Fura2FF and Fura6F

Several studies on $[Ca^{2+}]$ in nerve terminals have used Fura6F. Estimates for its K_D range from 5.3 μM (Life Technologies) to 15 μM (Müller *et al.* 2007). Fura6F is no longer available commercially and will probably be replaced by Fura2FF in future studies, as the K_D values of the two indicator dyes are very similar. We therefore considered it as important to compare the $K_{0.5}$ values of the two dyes, using the same method. We performed titrations on those solutions, which had actually been used in patch clamp experiments (KCl-based, potassium gluconate-based and caesium gluconate-based). We found a $K_{0.5}$ value for Fura6F in KCl-based solution of 17.8 μM. Values in gluconate$^-$-based solution including nucleotides were 56.2 and 84.5 μM for K^+ and Cs^+, respectively. Measurements with Fura6F confirmed the conclusion regarding contamination as obtained with Fura2FF.

Discussion

Here we characterize the Ca^{2+} binding properties of electrolyte solutions, as they are typically used in pipettes during whole cell patch clamp experiments on brain slices and neuronal cultures (adjusted to an ionic strength of 190 mM, pH 7.2, and at 22°C). We also determine stoichiometric (or concentration-based) dissociation constants for the Ca^{2+} indicator dyes Fura2FF and Fura6F.

The fluorimetric titrations presented do not rely on known dissociation constants of other Ca^{2+} buffers, only on the accuracy of a commercially available Ca^{2+} standard. In our measurements, we find that the $K_{0.5}$ of Fur2FF varies somewhat, depending on the major anion used, as expected from the physical chemistry of electrolyte solutions (Harned & Owen, 1958). These variations range from 10 to 20% for chloride, glutamate, methanesulfonate and isethionate (see Table 1). Gluconate-based solutions, however, have $K_{0.5}$ values that are higher by about a factor of 2–3. Since our method measures the product

Figure 3. Effects of excess ATP^{2-} and Mg^{2+} on the $K_{0.5}$ of Fura2FF
Titration curves for solutions with 100 mM caesium gluconate under normal conditions as well as in the presence of excess ATP or Mg^{2+} are indicated by the solid, dashed and dotted lines, respectively. Fitting the bound fraction of Fura2FF from three measurements of each solution yielded $K_{0.5}$ values of 65.5 ± 3.2 μM for the normal solution, 229.2 ± 3.9 μM for the solution with excess ATP and 49.0 ± 2.3 μM for the solution with excess Mg^{2+}.

of the actual K_D and the combined Ca^{2+} binding ratio, κ, of all low-affinity Ca^{2+} ligands present, we interpret the higher values for gluconate-based solutions in terms of low-affinity Ca^{2+} binding of the glutamate anion (Christoffersen & Skibsted, 1975). Furthermore, we find that nucleotides, such as ATP^{2-} and GTP^{2-}, also contribute to the Ca^{2+} binding capacity. This contribution varies strongly with the presence of magnesium, which competes for nucleotide binding.

Together, the contributions of gluconate and nucleotides to κ (the ratio of total Ca^{2+} over free Ca^{2+}) may range from 1.5 to 15. This can have substantial effects on Ca^{2+} buffering, given estimates for total Ca^{2+} binding ratio, κ_s, of fixed low-affinity buffers in the cytoplasm of Calyx nerve terminals ranging from 25 to 40 and considering the high Ca^{2+} binding rate of ATP^{2-} ($>10^9$ M^{-1} s^{-1}; theoretical 8×10^9 M^{-1} s^{-1} (Hammes & Levison, 1964)). In fact, we find that Ca^{2+} influx is 2.7 times less efficient in triggering neurotransmitter release in Calyx of Held nerve terminals with a caesium gluconate solution with 3 mM free $[ATP^{2-}]$ than with a caesium methanesulfonate-based solution with negligible Ca^{2+} binding capacity. As ATP^{2-} and Mg^{2+} may vary widely in the cytoplasm, depending on the metabolic state

of the cells (Veech *et al.* 1979), this demonstrates that their balance needs careful consideration.

Comparison with literature data

Our value of K_D for Fura2FF in KCl-based solutions without nucleotides (13.8 ± 1.1 μM) does not compare favourably with 5 μM reported by Xu-Friedman & Regehr (1999) and 4.18 μM by Aponte *et al.* (2008). Values for both dyes are also quite different from those given by the suppliers (LifeTech: Fura6F $K_D = 5.30$ μM, TefLabs: Fura2FF $K_D = 35$ μM). This discrepancy is probably due to differences in ionic strength and assumptions about the K_D of calibration buffers. However, when extrapolating our K_D to an ionic strength of 100 mM, ($K_{0.5} = -6.891 \times 10^{-6} + 1.09 \times 10^{-4}$ I) a more comparable K_D is estimated (~ 3.58 μM). Our K_D of 17.8 ± 1.3 μM for Fura6F data is in rather good agreement with the 15 μM reported by Müller *et al.* (2007).

We confirm that gluconate has some Ca^{2+} binding capacity. At a concentration of 100 mM, its contribution to the Ca^{2+} binding ratio (1.75) suggests a K_D of 57 mM, which is much higher than the reported 15.5 mM (Skibsted & Kilde, 1972). However, a more recent study reported K_D
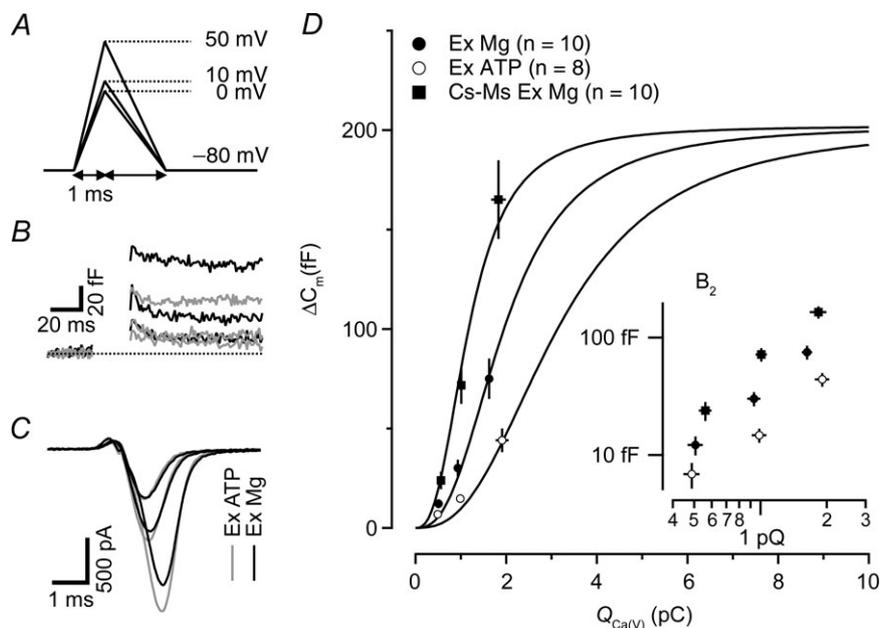
Figure 4. A pronounced shift in the capacitance – presynaptic Ca^{2+} charge relationship in the presence of excess free ATP
A, a series of AP-like voltage ramps (-80 to 50, 10 and 0 mV with depolarization phase, 1 ms and repolarization phase 2 ms) were applied to calyx terminals. *B* and *C*, averaged capacitance traces and Ca^{2+} currents were obtained from 10, 8 and 10 terminals with Ex ATP (black), Ex Mg (grey) and methanesulfonate (not shown in *A*–*C* for clarity of display), respectively. *D*, changes in capacitance as functions of presynaptic Ca^{2+} charge. The smooth black lines represent fits to the data using a Hill equation with midpoint at 1.18 pC (methanesulfonate), 1.97 pC (Ex Mg) and 3.16 pC (Ex ATP). The maximum for the Hill-fit was fixed to 202.2 fF, which is the mean of responses to 10 mV step depolarizations to 0 mV (257.9 fF for methanesulfonate, 169.4 fF for gluconate with excess Mg^{2+} and 180.2 fF for gluconate with excess ATP). The inset figure presents the relationship with double-logarithmic scale. Note the clear shifts along the *x*-axis between the three curves.

values of 32.3 and 71.4 mM from calcium electrode-based measurements and iodometric titrations in 0.2 M NaCl, respectively (Vavrusova *et al.* 2013). Likewise, the increase in $K_{0.5}$ by 13.85 μM for the iKCl solution with 3.3 mM free nucleotides indicates a K_D for Ca^{2+} binding to ATP^{2-} of 0.24 mM, which is very close to the 0.2 mM reported by Schoenmakers *et al.* (1992). The $K_{0.5}$ measured for the glutamate solution was found to be only slightly greater than the K_D of the calcium indicator, and thus we cannot confirm significant Ca^{2+} binding to glutamate$^-$, as reported by Davies & Waind (1950).

Comparison with other calibration methods

The method for calibrating Ca^{2+} indicator dyes, described here, has the advantage that it does not rely on any other Ca^{2+} buffer and can be readily performed with solutions actually used for filling patch clamp pipettes. Its disadvantage is that it does not discriminate between loose electrostatic interactions and specific, low-affinity binding. We have to infer the latter by the assumption that the true dissociation constant of the indicator dye in the presence of a given Ca^{2+} binding anion is the same as that in the presence of a similar anion without Ca^{2+} binding properties.

In our analysis we decomposed the excitation spectra, measured from the titration samples using a spectrofluorometer, as linear combinations of spectra from Ca^{2+}-free and Ca^{2+}-saturated samples of the dye. The corresponding fractional contributions are equated with the free and bound fractions of dye, respectively. Alternatively, one may perform calibrations under the fluorescence microscope with glass capillaries with short path lengths (e.g. 350 μm), in which it is more practical to perform measurements with two excitation wavelengths, and analyse data according to

$$[Ca^{2+}] = K'_{eff} \cdot (R - R_{min})/(R_{max} - R), \quad (9)$$

as originally described by Grynkiewicz *et al.* (1985). This uses calibration parameters R_{min} (ratio at zero [Ca^{2+}]), R_{max} (ratio at saturating [Ca^{2+}]) and an effective K'_{eff}.

When using Ca^{2+}-indicator dyes, such as Fura2FF or Fura6F on the microscope, one has to calibrate the dye for ratiometric use. Given the knowledge of the actual (instrument-independent) value of the K_D (e.g. for iKCl), we propose the following strategy to render the ratiometric calibration consistent with K_D.

- Determine R_{min} and R_{max} using a medium dye concentration of 200 μM and either *in vitro* or *in vivo* calibration procedures, as described previously (Helmchen, 2005; Neher, 2005; Schneggenburger, 2005).

- Determine the value of α (iso-coefficient), for which $F_1 + \alpha F_2$ (F_1 and F_2 being fluorescence values at excitation wavelengths 1 and 2, respectively) does not change during a [Ca^{2+}] transient (Zhou & Neher, 1993).

From this, an estimate of K_{eff} of the indicator dye can be obtained using the equation

$$K'_{eff} = K_D \cdot (R_{min} + a)/(R_{max} + a) \quad (10)$$

to be used for ratiometric measurements eqn (9). Alternatively, a full ratiometric calibration with three or more calibration solutions (see, for instance, Schneggenburger, 2005) yields values for R_{min}, R_{max} and K_{eff}. Determining the isocoefficient then allows one to calculate K_D from eqn (10). This value should agree with the one determined by the spectroscopic calibration (for KCl-based solutions without nucleotides). Deviations between the two values may be due to procedural errors, incorrect assumptions about the K_D of the buffer used, or differences between the *in vitro* situation and the intra-cellular environment during an *in vivo* calibration (for details see Helmchen, 2005; Neher, 2005). We compared the K_D values of our 'spectroscopic' calibration of Fur6F in isotonic KCl with that of an *in vivo* calibration of the same dye in caesium gluconate-based solution and found $K_{D,spec} = 17.8 \pm 1.3$ μM and $K_{D,in\text{-}situ} = 12.9 \pm 0.1$ μM. For the *in vivo* calibration we used DPTA as a calibration buffer (Schneggenburger, 2005) assuming a K_D of 80 μM. The small discrepancy is expected, given the range of K_D values observed *in vitro* for different anions and given the fact that the ionic milieu in the crowded environment of the cytoplasm is definitely not the same as that of a relatively dilute aqueous solution (Poenie, 1990).

Choice of anions in whole cell patch clamp experiments

We find that gluconate adds 1.75 to the Ca^{2+} binding capacity of the pipette solution and nucleotides (4 mM MgATP + 0.3 mM NaGTP) add another 1.8 to this number. The combined effect is negligible for many situations, given the intrinsic fixed buffer capacity of most neurons ranging from 20 to hundreds. On the other hand, little is known about mobile endogenous Ca^{2+} binding molecules, which may include Ca^{2+} binding proteins, nucleotides and other low molecular-weight substances that may be replaced by constituents of the pipette solution (Müller *et al.* 2007). If endogenous mobile Ca^{2+} buffers are scarce, the apparent diffusion coefficient of Ca^{2+} may change several fold (Wagner & Keizer, 1994; Neher, 1998) when pipette-delivered mobile buffers compete with fixed buffers and thereby mobilize Ca^{2+}. Also, calculations of microdomain Ca^{2+} signals are expected to be strongly influenced by low-affinity binding

of ATP^{2-} or gluconate. Given the high concentrations of these reagents, the binding product (product of anion concentration and Ca^{2+} binding rate constant, k_{on}) may be very high. Although no data seem to be available for k_{on} of gluconate, a typical value of 10^8 M^{-1} s^{-1} combined with a concentration of 0.1 M will result in 10^7 s^{-1}. This, together with a diffusion coefficient D_{Ca} of 220 μm^2 s^{-1} results in a length constant for diffusional equilibration of $\sqrt{D_{Ca}/10^7} \approx 4.7$nm (Neher, 1998). This implies that within 10 nm of a Ca^{2+} source, free Ca^{2+} will be equilibrated with gluconate. Given the Ca^{2+} binding ratio of the solution discussed, the free $[Ca^{2+}]$ will be reduced by a factor of 2.75 by gluconate and by a factor of 4.55 for the combined effect of gluconate and nucleotides. Given the steep dependence of neurotransmitter release on $[Ca^{2+}]$, this should have dramatic consequences on release at synapses with very tight coupling between channels and Ca^{2+} sensors. Release at synapses with weaker coupling should not be influenced as much by the choice of anions, since slower buffers with higher affinity are expected to control $[Ca^{2+}]$ at larger distances (Naraghi & Neher, 1997). The relatively modest effects observed in our measurements at the Calyx of Held are consistent with larger coupling distances, as reported for this preparation (Wang *et al.* 2008). In this sense, comparisons of release between methanesulfonate and gluconate or else while varying the Mg^{2+}/ATP ratio should be good indicators for very tight coupling between release-ready vesicles and Ca^{2+} channels, such as those found at cochlear hair cells (Wong *et al.* 2014).

References

Adler EM, Augustine GJ, Duffy SN & Charlton MP (1991). Alien intracellular calcium chelators attenuate neurotransmitter release at the squid giant synapse. *J Neurosci* **11**, 1496–1507.

Aponte Y, Bischofberger J & Jonas P (2008). Efficient Ca^{2+} buffering in fast-spiking basket cells of rat hippocampus. *J Physiol* **586**, 2061–2075.

Arslan P, Di Virgilio F, Beltrame M, Tsien RY & Pozzan T (1985). Cytosolic Ca^{2+} homeostasis in Ehrlich and Yoshida carcinomas. A new, membrane-permeant chelator of heavy metals reveals that these ascites tumor cell lines have normal cytosolic free Ca^{2+}. *J Biol Chem* **260**, 2719–2727.

Bates DM & Watts DG (2008). *Nonlinear Regression Analysis and Its Applications*. John Wiley & Sons, New York.

Bers DM, Patton CW & Nuccitelli R (1994). A practical guide to the preparation of Ca^{2+} buffers. *Methods Cell Biol* **40**, 3–29.

Bockris JOM & Reddy AKN (1973). *Modern Electrochemistry*, Vol. **1**. Plenum Press, New York.

Bonate PL (2011). *Modeling, Pharmacokinetic-pharmacodynamic*. Springer, New York.

Christoffersen GRJ & Skibsted LH (1975). Calcium ion activity in physiological salt solutions: influence of anions substituted for chloride. *Comp Biochem Physiol A Comp Physiol* **52**, 317–322.

Davies CW & Waind GM (1950). The extent of dissociation of salts in water. Part XII. Calcium salts of some amino-acids and dipeptides. *J Chem Soc*, 301–303.

Dodge FA Jr & Rahamimoff R (1967). Co-operative action a calcium ions in transmitter release at the neuromuscular junction. *J Physiol* **193**, 419–432.

Eggermann E, Bucurenciu I, Goswami SP & Jonas P (2011). Nanodomain coupling between Ca^{2+} channels and sensors of exocytosis at fast mammalian synapses. *Nature Rev Neurosci* **13**, 7–21.

Grynkiewicz G, Poenie M & Tsien RY (1985). A new generation of Ca^{2+} indicators with greatly improved fluorescence properties. *J Biol Chem* **260**, 3440–3450.

Hammes GG & Levison SA (1964). A kinetic investigation of the interaction of adenosine-5'-triphosphate with divalent metal ions. *Biochemistry* **3**, 1504–1506.

Harned HS & Owen BB (1958). *The Physical Chemistry of Electrolyte Solutions*. Reinhold Book Corp., New York.

Harrison SM & Bers DM (1989). Correction of proton and Ca association constants of EGTA for temperature and ionic strength. *Am J Physiol* **256**, C1250–1256.

Helmchen F (2005). Calibration of fluorescent calcium indicators. *Cold Spring Harbor Protoc* **2005**, 253.

Lakowicz JR (2006). *Principles of Fluorescence Spectroscopy*. Springer, New York.

Lin KH, Erazo-Fischer E & Taschenberger H (2012). Similar intracellular Ca^{2+} requirements for inactivation and facilitation of voltage-gated Ca^{2+} channels in a glutamatergic mammalian nerve terminal. *J Neurosci* **32**, 1261–1272.

Lin KH, Oleskevich S & Taschenberger H (2011). Presynaptic Ca^{2+} influx and vesicle exocytosis at the mouse endbulb of Held: a comparison of two auditory nerve terminals. *J Physiol* **589**, 4301–4320.

Martell A & Smith R (1974). *Critcal Stability Constants*. Plenum Press, New York.

Moisescu DG & Thieleczek R (1979). Sarcomere length effects on the Sr^{2+}- and Ca^{2+}-activation curves in skinned frog muscle fibres. *Biochim Biophys Acta* **546**, 64–76.

Müller M, Felmy F, Schwaller B & Schneggenburger R (2007). Parvalbumin is a mobile presynaptic Ca^{2+} buffer in the Calyx of Held that accelerates the decay of Ca^{2+} and short-term facilitation. *J Neurosci* **27**, 2261–2271.

Naraghi M & Neher E (1997). Linearized buffered Ca^{2+} diffusion in microdomains and its implications for calculation of $[Ca^{2+}]$ at the mouth of a calcium channel. *J Neurosci* **17**, 6961–6973.

Neher E (1998). Usefulness and limitations of linear approximations to the understanding of Ca^{++} signals. *Cell Calcium* **24**, 345–357.

Neher E (2005). Some quantitative aspects of calcium fluorimetry. *Cold Spring Harbor Protoc* **2005**, 245.

Neher E & Taschenberger H (2013). Transients in global Ca^{2+} concentration induced by electrical activity in a giant nerve terminal. *J Physiol* **591**, 3189–3195.

Poenie M (1990). Alteration of intracellular Fura-2 fluorescence by viscosity: a simple correction. *Cell Calcium* **11**, 85–91.

Robinson RA & Stokes RH (1959). *The Measurement and Interpretation of Conductance, Chemical Potential and Diffusion in Solutions of Simple Electrolytes.* Butterworths, London.

Schneggenburger R (2005). Ca^{2+} unaging in nerve terminals. In *Imaging in Neuroscience and Development.* CSHL, Woodbury, NY.

Schoenmakers TJ, Visser GJ, Flik G & Theuvenet AP (1992). CHELATOR: an improved method for computing metal ion concentrations in physiological solutions. *BioTechniques* **12**, 870–874, 876–879.

Skibsted LH & Kilde G (1972). Dissociation constant of calcium gluconate. Calculations from hydrogen ion and calcium ion activities. *Dan Tidsskr Farm* **46**, 41–46.

Vavrusova M, Munk MB & Skibsted LH (2013). Aqueous solubility of calcium L-lactate, calcium D-gluconate, and calcium D-lactobionate: importance of complex formation for solubility increase by hydroxycarboxylate mixtures. *J Agric Food Chem* **61**, 8207–8214.

Veech RL, Lawson JW, Cornell NW & Krebs HA (1979). Cytosolic phosphorylation potential. *J Biol Chem* **254**, 6538–6547.

Wagner J & Keizer J (1994). Effects of rapid buffers on Ca^{2+} diffusion and Ca^{2+} oscillations. *Biophys J* **67**, 447–456.

Wang L-Y, Neher E & Taschenberger H (2008). Synaptic vesicles in mature Calyx of Held synapses sense higher nanodomain calcium concentrations during action potential-evoked glutamate release. *J Neurosci* **28**, 14450–14458.

Wong AB, Rutherford MA, Gabrielaitis M, Pangršič T, Göttfert F, Frank T, Michanski S, Hell S, Wolf F, Wichmann C & Moser T (2014). Developmental refinement of hair cell synapses tightens the coupling of Ca^{2+} influx to exocytosis. *EMBO J* **33**, 247–264.

Xu-Friedman MA & Regehr WG (1999). Presynaptic strontium dynamics and synaptic transmission. *Biophys J* **76**, 2029–2042.

Zhou Z & Neher E (1993). Mobile and immobile calcium buffers in bovine adrenal chromaffin cells. *J Physiol* **469**, 245–273.

Additional information

Competing interests

The authors have no conflicts of interest to declare.

Author contributions

A.W., K.H.L. and E.N. conceived and designed the research; A.W. and K.H.L. performed the experiments; A.W., K.H.L. and E.N. analysed the data; A.W. and E.N. wrote the manuscript. All authors approved the final version.